

NATURAL FREQUENCIES OF AN ORBITING SPACE STATION

Edward L. Bernstein

May 8, 1972

Backup Document for AIAA Synoptic Scheduled for  
Publication in the Journal of Spacecraft and Rockets

September 1972

Applied Dynamics Research  
Corporation  
3313 Memorial Parkway, S. W.  
Huntsville, Alabama 35801

(NASA-CR-123557) NATURAL FREQUENCIES OF AN  
ORBITING SPACE STATION E.L. Bernstein N72-24922  
(Applied Dynamics Research Corp.) 8 May  
1972 30 p CACL 22B  
Unclas  
G3/31 28221

Reproduced by  
NATIONAL TECHNICAL  
INFORMATION SERVICE  
U S Department of Commerce  
Springfield VA 22151

## ACKNOWLEDGMENTS

This study was supported by NASA Contract NAS8-20082. The author is grateful to L. A. Kiefling of NASA for his support while monitoring the task, and to the following Lockheed associates: K. R. Leimbach for many helpful suggestions; W. D. Whetstone for guidance; and F. D. Tebbenkamp who performed much of the numerical work.

## ABSTRACT

The technique of modal synthesis is applied to find the natural frequencies of space stations. The station is modeled as an assemblage of rigid modules, joined by massless elastic constraints, and flexible modules characterized by deformation functions. The equations of motion are derived and system mass and stiffness matrices derived. The method is applied to the Skylab orbiting space station. The frequencies of the lowest 65 modes are given and selected mode shapes illustrated. The technique is feasible for analysis of a complex system and suitable for response studies including damping and attitude control system effects.

## NOMENCLATURE

$a_n$	coefficient of deformation function
B	body
K, $K_{mn}$	stiffness matrix and submatrices
$\underline{l}_i$	position vector of origin of secondary rigid module frame
M, $M_{mn}$	mass matrix and submatrices
$\underline{q}$	row vector of generalized coordinates
$\underline{r}$	displacement vector
$\underline{s}_j$	position vector of origin of frame in flexible module
T, V	kinetic and potential energy
$\underline{x}$	position vector of mass point in flexible module
$\underline{y}$	elastic displacement vector
$\underline{\theta}$	rotation vector of rigid module
$\underline{\psi}_n$	deformation function
$\underline{\omega}$	angular velocity
<u>Subscripts</u>	
i	secondary rigid module
j	flexible module
o	primary rigid module

# NATURAL FREQUENCIES OF AN ORBITING SPACE STATION

Edward L. Bernstein\*

Applied Dynamics Research Corporation, Huntsville, Ala.

## Introduction

Because of their structural complexity, space stations present difficulties for the traditional methods of vibrational analysis. The large number of members in these structures present a challenge for accurate mathematical modeling in order that digital computer techniques may be applied with reasonable core storage requirements and execution times. In addition, space stations are typically composed of structural modules with widely varying flexibilities. Long arrays of solar cell units are attached to relatively massive space vehicles. This situation can lead to numerical inaccuracy in the solution procedure. The formulation of the problem must avoid the pitfall of overshadowing the stiffness properties of the more flexible members by the stiff members. In addition, the choice of generalized coordinates for the model must be made so that low-frequency behavior is accurately described without using too many of the number of available degrees of freedom for higher frequency motion of the stiff members.

This paper presents a vibration analysis of a large space station. A number of papers have appeared on methods of analysis for structural systems (for example Ref. 1). However, the literature on the actual solution of a complex three-dimensional system with many components appears to be sparse. In Ref. 2 an analysis of a cruciform satellite, consisting of a hub with four cantilevered solar arrays, is given. The present paper discusses the solution for the modes and frequencies of a space station consisting of a number of clustered modules with appended flexible structures. The solution is given for a particular configuration of three modules with seven attached elastic structures.

In modal synthesis methods component or substructure displacement functions are used to model the entire assembly. In applying modal synthesis

---

\*Research Specialist in Structural Dynamics. The paper describes work done under NASA Contract NAS8-20082 while the author was an employee of Lockheed Missiles & Space Co., Huntsville, Ala/

to space stations, the key to formulating a model of manageable size which will accurately represent low-frequency behavior is the proper selection of substructure displacement functions to use as generalized coordinates of the system.

The assumption was made that the space station consisted of both rigid and flexible modules, interfacing at planar surfaces. This assumption is suitable for clustered space structures where the requirements of small launch volume lead to docking and deployment of modules and subsystems, so that interfacing is confined to localized areas. For such a situation it is a valid approximation to consider the flexibility lumped at the interface. The rigid substructures are characterized by natural frequencies well above the highest frequency of interest for the complete space station model. The deformation functions for these bodies are the six rigid-body motions.

The flexible substructures are restricted to cantilevered structures characterized by low frequencies, such as deployable solar arrays. The deformation functions for these bodies are elastic displacement functions, such as natural mode shapes or static responses to inertia loads.

#### Formulation of the Equations of Motion

From the preceding discussion it is apparent that the generalized coordinates used to describe the motion of the space station will be either rigid-body modes of modules or coefficients of displacement functions. If the array of generalized coordinates is represented by the column matrix  $\mathbf{q}$ , then the kinetic energy and the potential energy of the space station are given by

$$T = \frac{1}{2} \dot{\mathbf{q}}^T \mathbf{M} \dot{\mathbf{q}} \quad (1a)$$

$$V = \frac{1}{2} \mathbf{q}^T \mathbf{K} \mathbf{q} \quad (1b)$$

The elements of  $\mathbf{M}$  and  $\mathbf{K}$  are assumed constant. This assumption is reasonable for obtaining short-term vibrational behavior after earth orbit is obtained. When there are no applied forces or dissipative effects,

Lagrange's equation yields

$$\mathbf{M} \ddot{\mathbf{q}} + \mathbf{K} \mathbf{q} = 0 \quad (2)$$

An assumed harmonic solution of the form

$$\mathbf{q} = \mathbf{u} \sin \omega t \quad (3)$$

where  $\mathbf{u}$  is a function of spatial variables, gives the linear eigenvalue problem

$$\omega^2 \mathbf{M} \mathbf{u} - \mathbf{K} \mathbf{u} = 0 \quad (4)$$

### Generalized Coordinates

One of the rigid bodies comprising the space station model is designated as the primary module. A reference frame is fixed in it, with the displacement and rotation of its origin described by  $\mathbf{r}_0, \theta_0$  with respect to inertial space (see Fig. 1). A frame fixed in the  $i$ -th secondary rigid module has displacement and rotation vectors  $\mathbf{r}_i, \theta_i$ , defining motion relative to the primary module. These coordinates describe the elastic motion of these bodies, assuming they are attached to the primary module by massless elastic constraints. The origin of each frame before deformation is located relative to the origin of the main frame by  $\mathbf{L}_i$ .

Reference frames for the flexible structures are established with their origins at the interface between the flexible module and its supporting rigid module. These frames are fixed in the rigid module and located in the rigid module frame by  $\mathbf{S}_j$  (see Fig. 1). A point within the flexible module is located by  $\mathbf{x}$  in the frame for the flexible structure. Its displacement due to elastic deformation is specified by  $\mathbf{y}(\mathbf{x})$  where

$$\mathbf{y} = \sum_n a_n \varphi_n(\mathbf{x}_j) \quad (5)$$

In this expression the  $\varphi_n(\mathbf{x})$  are deformation functions of the flexible

component, such as natural mode shapes or static response to inertia loading; the  $a_n$  are constant coefficients. The summation is over the total number of functions characterizing the  $j$ -th flexible module.

Therefore, the generalized coordinates for the complete space station system are the components  $r_{on}, \theta_{on}$  ( $n=1,2,3$ ) of the rigid-body motion of the primary module, the components  $(r_{in}, \theta_{in}, n=1,2,3)$  of motion of the secondary rigid modules and the coefficients  $a_n$  of deformation functions for the flexible structures. They are written as a row matrix  $\mathbf{q}$ :

$$\mathbf{q} = [\underline{r}_o, \underline{\theta}_o, \underline{r}_i, \underline{\theta}_i, a_n] \quad (6)$$

### Kinetic and Potential Energy

The total kinetic energy and potential energy of the space station (Eqs. 1a, 1b) are derived as a summation of the energies of individual components.

The kinetic energy for a flexible component is written partly in terms of its deformation functions and partly in terms of rigid-body motion of the interface. The interface motion is not an independent coordinate, but is expressed in terms of the coordinates of the supporting module. The kinetic energy will be derived for a flexible component  $B_j$  interfacing with a rigid module  $B_i$  which, in turn, is attached to the free primary module  $B_o$ . This configuration is the case, for example, for a solar array wing on a module docked to another module as illustrated in Fig. 1.

The position vector  $\underline{r}$  of a point in  $B_j$  is

$$\underline{r} = \underline{r}_o + \underline{\ell}_i + \underline{r}_i + \underline{s}_j + \underline{x}_j + \underline{y}_j \quad (7)$$

The kinetic energy  $dT_j$  of the mass point in  $B_j$  is

$$dT_j = \dot{\underline{r}} \cdot \dot{\underline{r}} dm \quad (8)$$

where  $dm$  is the mass at the point and a superscripted dot here denotes inertial time derivative. Then



$$T_j = \int_{B_j} \dot{\mathbf{r}} \cdot \dot{\mathbf{r}} \, dm \quad (9)$$

In order to carry out the operations indicated in this equation, it is necessary to use the relationship between time derivatives of a vector in a fixed and a rotating frame. If there is a fixed frame and a frame which rotates with respect to it with an angular velocity  $\underline{\omega}$ , then a position vector  $\underline{a}$  of a point from the origin of the fixed frame may be written as

$$\underline{a} = \underline{b} + \underline{\omega} \times \underline{c} + \underline{\dot{c}}$$

where  $\underline{b}$  is a vector locating the origin of the rotating frame relative to the origin of the fixed frame and  $\underline{c}$  is a position vector in the rotating frame (see Fig. 2). The time derivative  $\underline{\dot{a}}$  in the fixed frame is then given by the formula

$$\underline{\dot{a}} = \underline{\dot{b}} + \underline{\dot{c}} \quad (10)$$

where  $\underline{\dot{b}}$  is a time derivative in the fixed frame and  $\underline{\dot{c}}$  is a time derivative in the rotating frame.

The velocity  $\dot{\mathbf{r}}$  may now be written from Eqs. (7) and (10) as

$$\dot{\mathbf{r}} = \dot{\mathbf{r}}_0 + \dot{\underline{\theta}}_0 \times \underline{\ell}_i + \dot{\mathbf{r}}_i + (\dot{\underline{\theta}}_0 + \dot{\underline{\theta}}_i) \times \underline{s}_j + (\dot{\underline{\theta}}_0 + \dot{\underline{\theta}}_i) \times \underline{x}_j + \sum_n \dot{a}_n \varphi_n(\underline{x}_j) \quad (11)$$

In this expression the convention for time derivatives has been used that superscripted dots denote derivatives with respect to the frame in which the vector is defined. Thus  $\dot{\mathbf{r}}_0$  is the inertial time derivative,  $\dot{\mathbf{r}}_i$  is in the frame in  $B_i$ , and  $\dot{a}_j$  is with respect to the frame associated with  $B_j$ . The angular velocity  $\dot{\underline{\theta}}_0$  expresses time rates of change of the orientation of  $B_0$  with respect to inertial space, and  $\dot{\underline{\theta}}_i$  expresses time rate of change with respect to  $B_0$ .

In the derivation of this expression the assumption of small deformations and angular rates has been used so that products of these terms have been neglected. Furthermore, this assumption permits us to identify the angular velocities,  $\dot{\underline{\theta}}_0$ ,  $\dot{\underline{\theta}}_i$ , directly as time rates of change of the angular orientation of the frame.

From Eqs. 7, 9, and 11, the kinetic energy  $T_j$  for component  $B_j$  may be formulated. The result is written as

$$T_j = \begin{bmatrix} \dot{r}_o \\ \dot{\theta}_o \\ \dot{r}_i \\ \dot{\theta}_i \\ \dot{a}_n \end{bmatrix}^T \begin{bmatrix} M_{11} & M_{12} & M_{13} & M_{14} & M_{15} \\ & M_{22} & M_{23} & M_{24} & M_{25} \\ & & M_{33} & M_{34} & M_{35} \\ \text{Symmetric} & & & M_{44} & M_{45} \\ & & & & M_{55} \end{bmatrix} \begin{bmatrix} \dot{r}_o \\ \dot{\theta}_o \\ \dot{r}_i \\ \dot{\theta}_i \\ \dot{a}_n \end{bmatrix} \quad (12)$$

In a similar way, the kinetic energy for each component of the entire system may be derived, and the total energy and system mass matrix formed by superposition.

While  $\mathbf{M}$  is relatively dense, the system stiffness matrix  $\mathbf{K}$  is relatively sparse. This characteristic is due to the definition of generalized coordinates relative to the system of embedded frames, since they allow expression of deformation within each component exclusive of rigid-body motion.

Formation of the stiffness matrix  $\mathbf{K}$  follows from derivation of the system potential energy  $V$ . The potential energy is in the form

$$V = \frac{1}{2} \begin{bmatrix} r_o \\ \theta_o \\ r_i \\ \theta_i \\ a_n \end{bmatrix}^T \begin{bmatrix} 0 & & 0 & & 0 \\ & & & & \\ 0 & & K_{33} & K_{34} & 0 \\ & & K_{34}^T & K_{44} & \\ 0 & & 0 & & K_{55} \end{bmatrix} \begin{bmatrix} r_o \\ \theta_o \\ r_i \\ \theta_i \\ a_n \end{bmatrix}$$

The submatrices of  $\mathbf{K}$  are of two types: those associated with rigid module motion, described by coordinates  $r_i$ ,  $\theta_i$ , and those associated with flexible module motion, described by coordinates  $a_n$  ( $n=1, \dots, N$ )

For the rigid modules the flexibility is considered to be localized at the interface with a supporting module. Then  $K_{33}$ ,  $K_{34}$  and  $K_{44}$  form a  $6 \times 6$  matrix of coefficients. These coefficients are determined from a separate static analysis of the localized interfacing structure, and represent the forces resisting unit displacements and rotations of the structure at one interface while it is fixed at the others.

The submatrix  $K_{55}$  corresponding to flexible module coordinates represents the coefficients of the potential energy of the flexible module. It is determined from a separate analysis of the module, in which the strain energy associated with the deflection function  $\varphi_n$  is found.

### Solution of the Equations

A general purpose digital computer program (DISCUS) was written for the synthesis of component modes for space stations, using the methodology described above. The program assembles the mass and stiffness matrices, and prepares the eigenvalue equation (4) for solution. The solution technique used for the eigenvalue equation was the Householder method (Ref. 3). The predominant substructure motion characterizing each system mode was found by computing the percentage of kinetic and potential energy in each substructure. The program also produced schematic diagrams illustrating each mode, using the Stromberg-Carlson 4020 plotter. The program was run on a Univac 1108 computer, Exec 8 system, with a 64,000 core capacity. The results reported here are for a model with a total of 96 degrees of freedom. Subsequently, the program was modified to allow 112 degrees of freedom.

### Application to the Skylab

The Skylab consists of several large structures in clustered configuration. As illustrated in Fig. 3, the Skylab contains a Saturn IV-B orbital workshop (OWS) which is the third stage of the Saturn launch vehicle converted for human habitation. The Airlock Module provides astronaut access

to the OWS through a flexible tunnel. The Airlock Module is mated to a Multiple Docking Adapter (MDA), a cylindrical shell structure with a forward conical bulkhead, providing forward and lateral docking ports for docking with the Command and Service Module (CSM). The CSM is a spacecraft bringing the returning astronauts to the Skylab. The CSM-MDA-AM-OWS form the main axis of the Skylab. At right angles to the main axis, pointing toward the sun, is the Apollo Telescope Mount (ATM). The ATM consists of a supporting structure and an experiment package, a rigid structure bearing a number of telescopic experiments for solar observation. The experiment package is attached with a gimballed ring system. The ATM is joined to the OWS with a Deployment Arm (DA), a pivoted truss system allowing the ATM to rotate into a sunward-pointing position after orbit. Four long articulated solar array wings are attached to the ATM, and the OWS supports two array systems, each with three wings.

A series of vibrational studies of the Skylab was made following the evolution of the design and configurational concepts. The results reported here are based on Ref. 4.

For the Skylab the selection of generalized coordinates was as follows:

Rigid Modules:

OWS/AM/MDA	6 degrees of freedom
ATM	6 degrees of freedom
CSM	6 degrees of freedom

Flexible Modules:

OWS Solar Arrays (2)	24 degrees of freedom each
ATM Solar Arrays (4)	6 degrees of freedom each
Canister (1)	6 degrees of freedom

Natural modes were used for all the flexible module deformation functions. The ranges of natural frequencies for the modules cantilevered at the interface with the space station are

OWS Solar Arrays	0.404-4.811 Hz
ATM Solar Arrays	0.224-2.696 Hz
Canister	1.192-7.730 Hz

The modes were found from finite element analyses of the structures. The ATM solar arrays and the canister were analyzed with the SNAP/Dynamics finite element program (Ref. 5), while the OWS solar array results are based on Ref. 6. The localized flexibility characterizing the rigid module interfaces is expressed in the form of 6 x 6 stiffness matrices. The coefficients of these matrices were found from static analyses with the SNAP finite element program.

All of the natural modes within the above ranges were used as module deformation functions. Truncation of the modes at the upper limits no doubt introduces some error. The highly separated nature of the Skylab modes found indicates that the given results are not significantly affected. Some additional solar array modes would have been present (and were indeed found subsequently) had the ATM solar array functions been truncated at a higher frequency.

Table 1 gives the mass data for the rigid modules. The results are given for the frequencies of the lowest 65 modes in Table 2. Computer run times were of the order of three minutes of CPU time for 96 modes, with about one and one-half additional minutes for plotting all modes. The modes are grouped according to the predominant component motion characterizing the mode. Illustrations of some of the mode shapes produced on the plotter are shown in Figs. 4-10.

All of the lowest 20 modes are predominantly solar array deformation. The spectrum of frequencies falls into groups of almost identical values because the Skylab has multiple solar arrays with nearly the same properties. Figures 4-8 illustrate these modes. The lowest mode characterized by motion of a rigid module is mode 21, 0.983 Hz (Fig. 9), which is predominantly twisting of the ATM about its longitudinal axis. The lowest mode of deformation of the main axis of the Skylab is mode 36, 1.424 Hz, characterized by bending of the CSM. This mode is illustrated in Fig. 10.

Through the modal synthesis method, a comprehensive analysis of a large space station is possible. The results indicate that generally the modes tend to fall into groups with relatively uncoupled motion of separate substructures. A tentative conclusion is that low-frequency motion of appendages may be neglected in studies of the gross motion of the main components.

The modal synthesis method as used here is adaptable for other types of analysis of space station motion. Damping effects, introduced as empirical modal damping coefficients, can be included. Response studies can be made using the mass, stiffness and damping matrices with standard computer numerical methods. The effects of control forces on short-term motion can also be included by including linearized control force laws in the system mass and damping matrices.

#### References

1. Benfield, W.A., and Hruda, R.F., "Vibration Analysis of Structures by Component Mode Substitution," AIAA Journal, Vol. 9, No. 7, July 1971, pp. 1255-1261.
2. Newton, J.K., and Farrell, J.L., "Natural Frequencies of a Flexible Gravity-Gradient Satellite," Journal of Spacecraft and Rockets, Vol. 5, No. 5, May 1968, pp. 560-569.
3. Wilkinson, J.H., The Algebraic Eigenvalue Problem, Oxford University Press, London, 1965.
4. Bernstein, E.L., "Natural Modes and Frequencies of the Skylab Cluster--December 1970," LMSC-HREC D162774, January 1971, Lockheed Missiles & Space Company, Huntsville, Ala.
5. Whetstone, W.D., and Jones, C.E., "Vibrational Characteristics of Linear Space Frames," Journal of the Structural Division, ASCE, Vol. 95, No. ST10, October 1969, pp. 2077-2091.
6. Lee, L.T., "Analytical Model of the Deployed Solar Array System," SAS-6-1733, June 18, 1970, Interoffice Correspondence, TRW Systems Group, Redondo Beach, Calif.

Table I  
 MASS PROPERTIES OF THE SKYLAB

Object	Weight (kg)	Moments of Inertia about Interface with Supporting Module (kg-sec <sup>2</sup> -m)		
		I <sub>xx</sub>	I <sub>yy</sub>	I <sub>zz</sub>
MDA/AM/OWS	58,252	36,716	345,231	347,093
ATM (with Deployment Arm, without Solar Arrays, Canister)	6,212	2,994	2,923	2,126
CSM	12,340	2,244	23,276	23,511
ATM Canister	2,745	407	415	177
ATM Solar Array (Typical)	368	1,027	1,027	2,026
OWS Solar Array System (Typical)	876	3,547	1,423	4,941

Table 2  
SKYLAB MODES AND FREQUENCIES

Mode	Frequency (Hz)	Description
1	.217	
2	.227	
3	.228	ATM Solar Array Bending
4	.232	
5	.382	
6	.384	OWS Solar Array Bending
7	.532	
8	.533	OWS Solar Array Twisting
9	.746	
10	.746	
11	.770	OWS Solar Array Bending
12	.770	
13	.801	
14	.836	
15	.841	ATM Solar Array Bending
16	.842	
17	.958	
18	.963	
19	.963	ATM Solar Array Twisting
20	.963	
21	.983	ATM Twisting
22	1.072	
23	1.086	
24	1.088	ATM Solar Array Bending
25	1.090	
26	1.095	
27	1.095	
28	1.102	
29	1.102	OWS Solar Array Twisting
30	1.102	
31	1.102	
32	1.185	Canister Rotation
33	1.314	
34	1.316	OWS Solar Array Bending
35	1.356	Canister Rotation
36	1.424	
37	1.485	CSM Rotation
38	1.604	
39	1.616	
40	1.622	ATM Solar Array Bending
41	1.628	
42	1.923	ATM Rotation

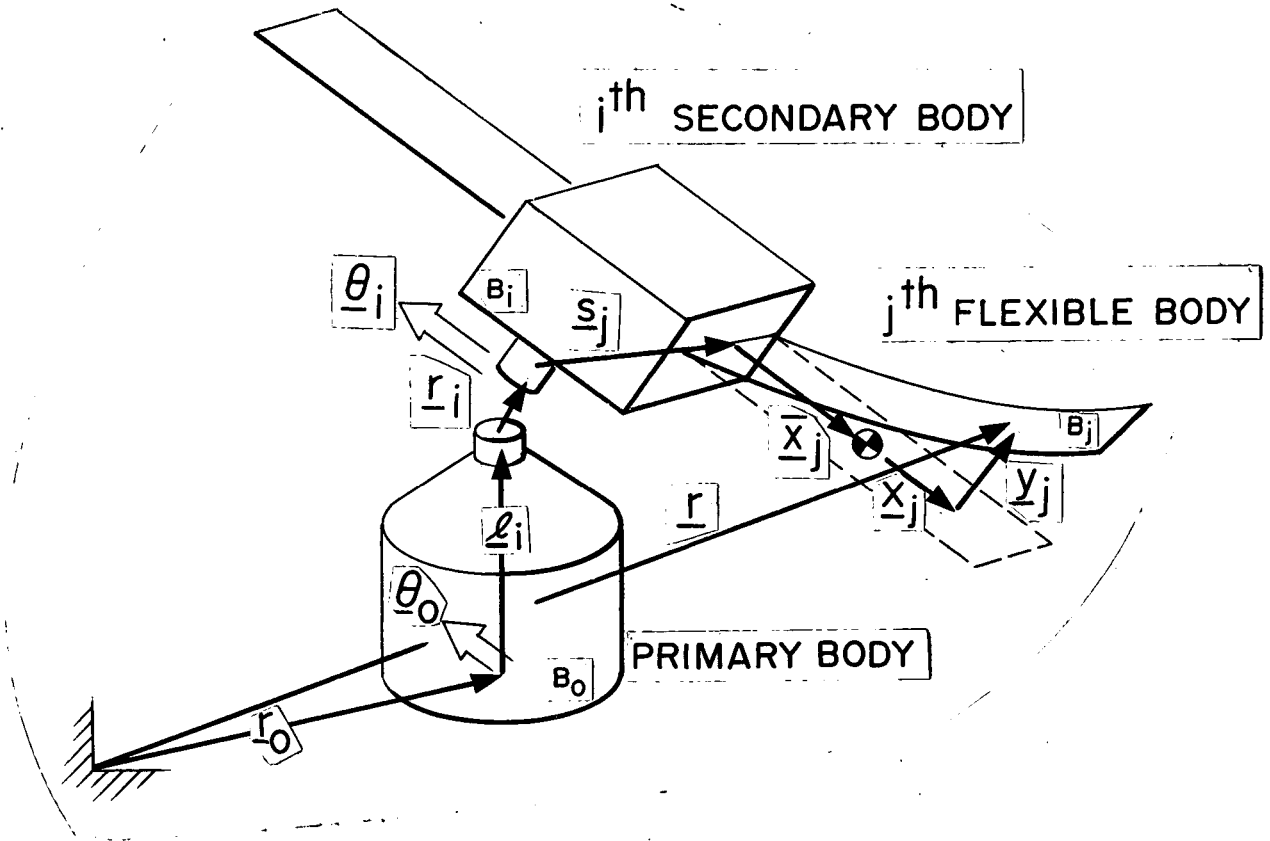


Table 2 (Continued)

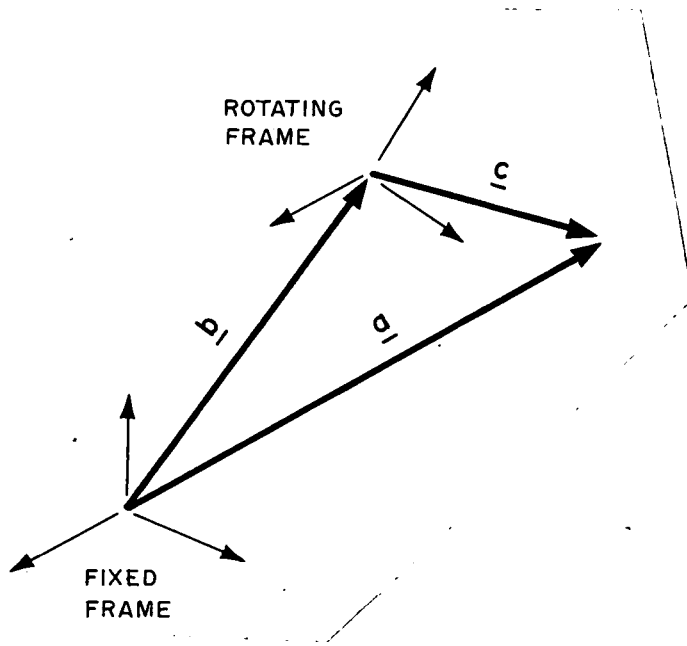
Mode	Frequency (Hz)	Description
43	2.338	OWS Solar Array Bending
44	2.341	
45	2.765	ATM Rotation
46	3.008	ATM Solar Array Twisting
47	3.009	
48	3.009	
49	3.010	
50	3.687	OWS Solar Array Bending
51	3.687	
52	4.072	Canister
53	4.321	OWS Solar Array Bending
54	4.326	
55	4.389	Canister Z-Translation
56	4.410	OWS Solar Array Bending
57	4.413	
58	4.471	
59	4.472	
60	4.797	OWS Solar Array Twisting
61	4.797	
62	4.801	
63	4.801	
64	4.811	
65	4.811	

## CAPTIONS

- Fig. 1 Model of Space Station Illustrating Generalized Coordinates
- Fig. 2 Coordinate Systems for Time Derivatives in a Rotating Frame
- Fig. 3 Schematic Diagram of the Skylab Space Station (three views)
- Fig. 4 Mode 1
- Fig. 5 Mode 5
- Fig. 6 Mode 7
- Fig. 7 Mode 9
- Fig. 8 Mode 13
- Fig. 9 Mode 21
- Fig. 10 Mode 36

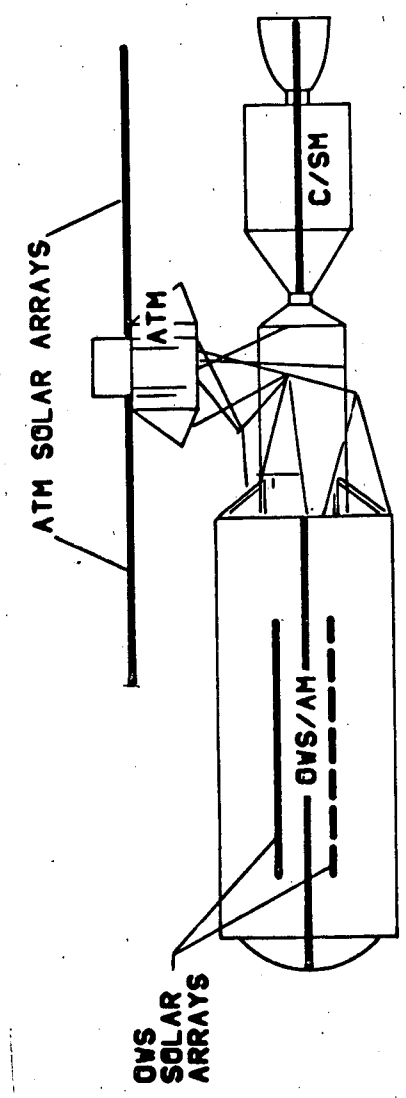
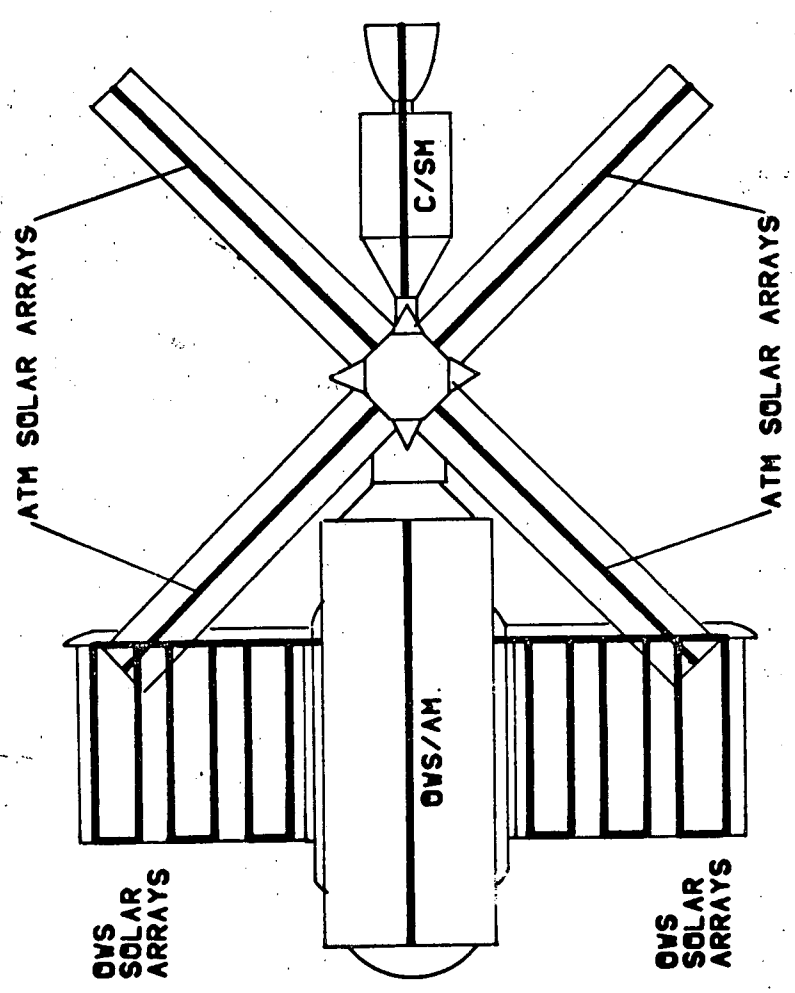
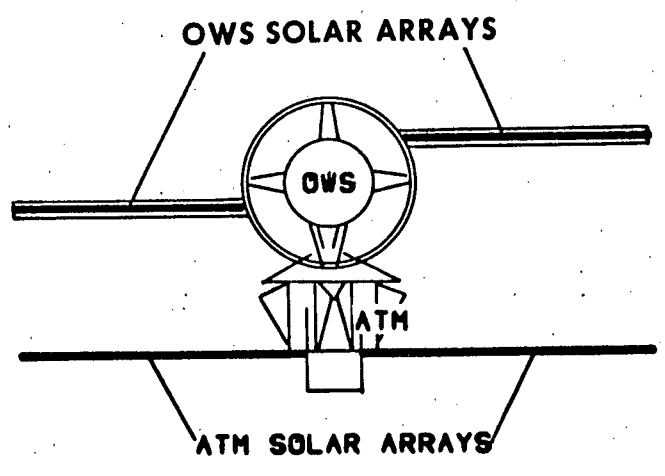


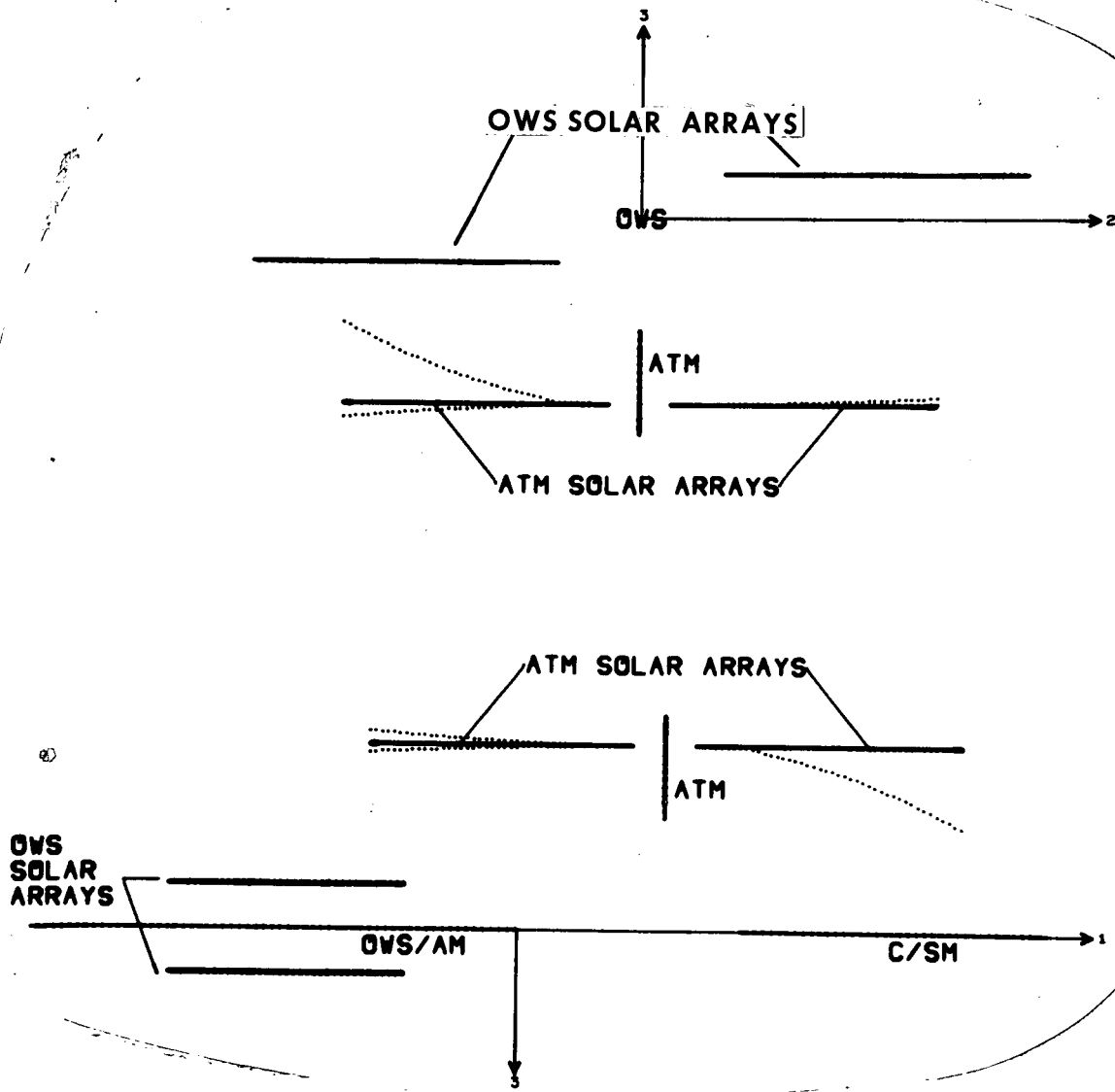
*E. L. Bernstein*  
 E. L. Bernstein  
 Fig. 1  
 16



E. L. Bernstein  
Fig. 2

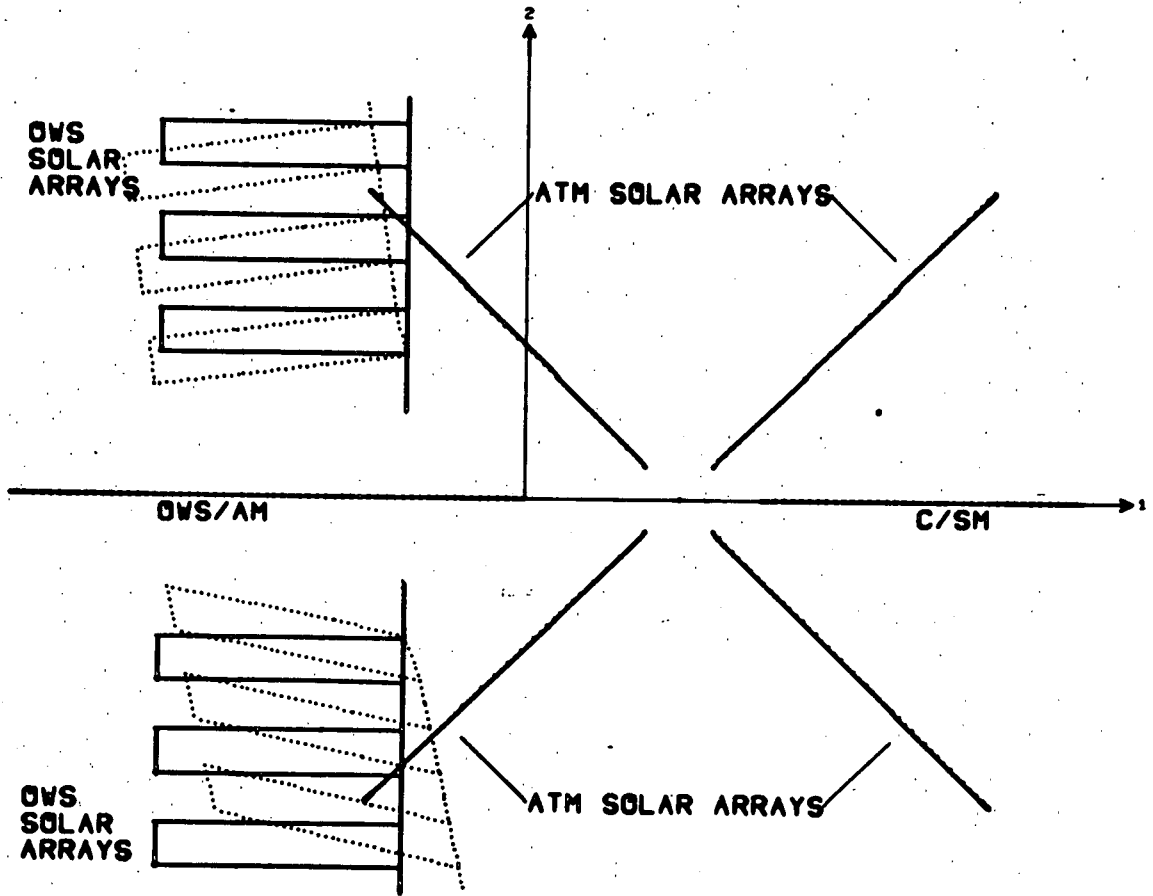
Fig 2



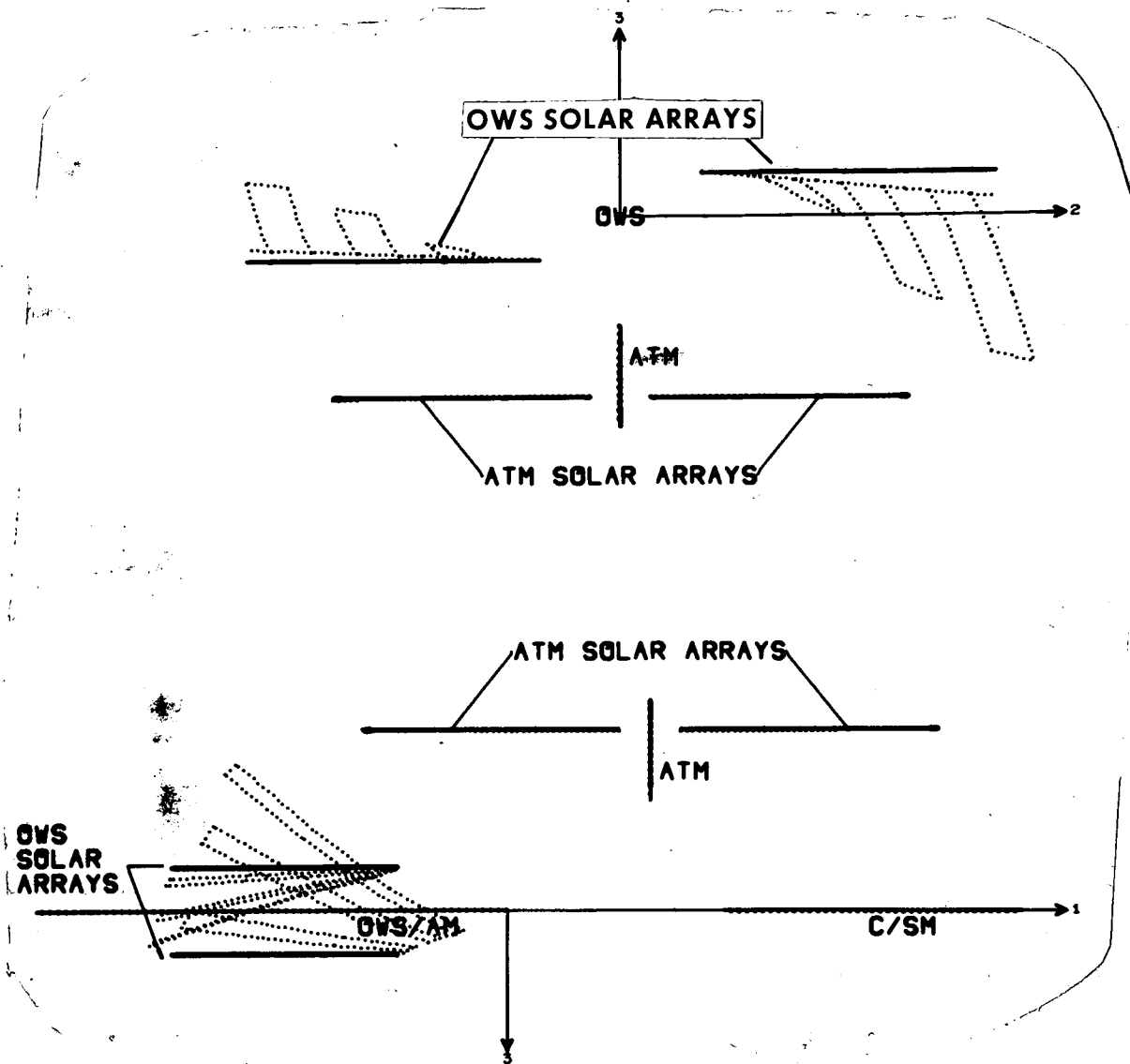


E. L. Bernstein

Fig. 4

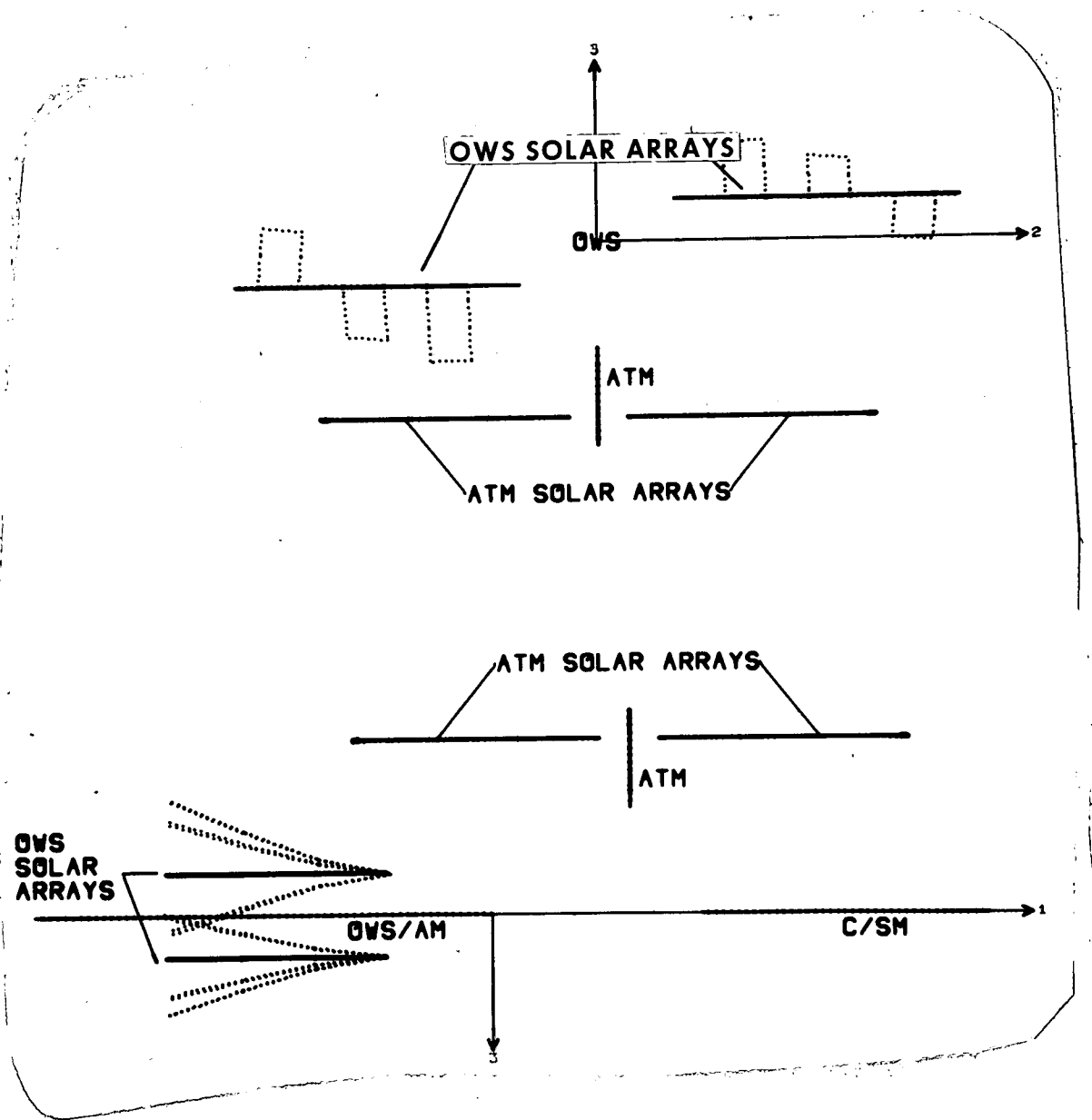


E. L. Bernstein  
 Fig. 5



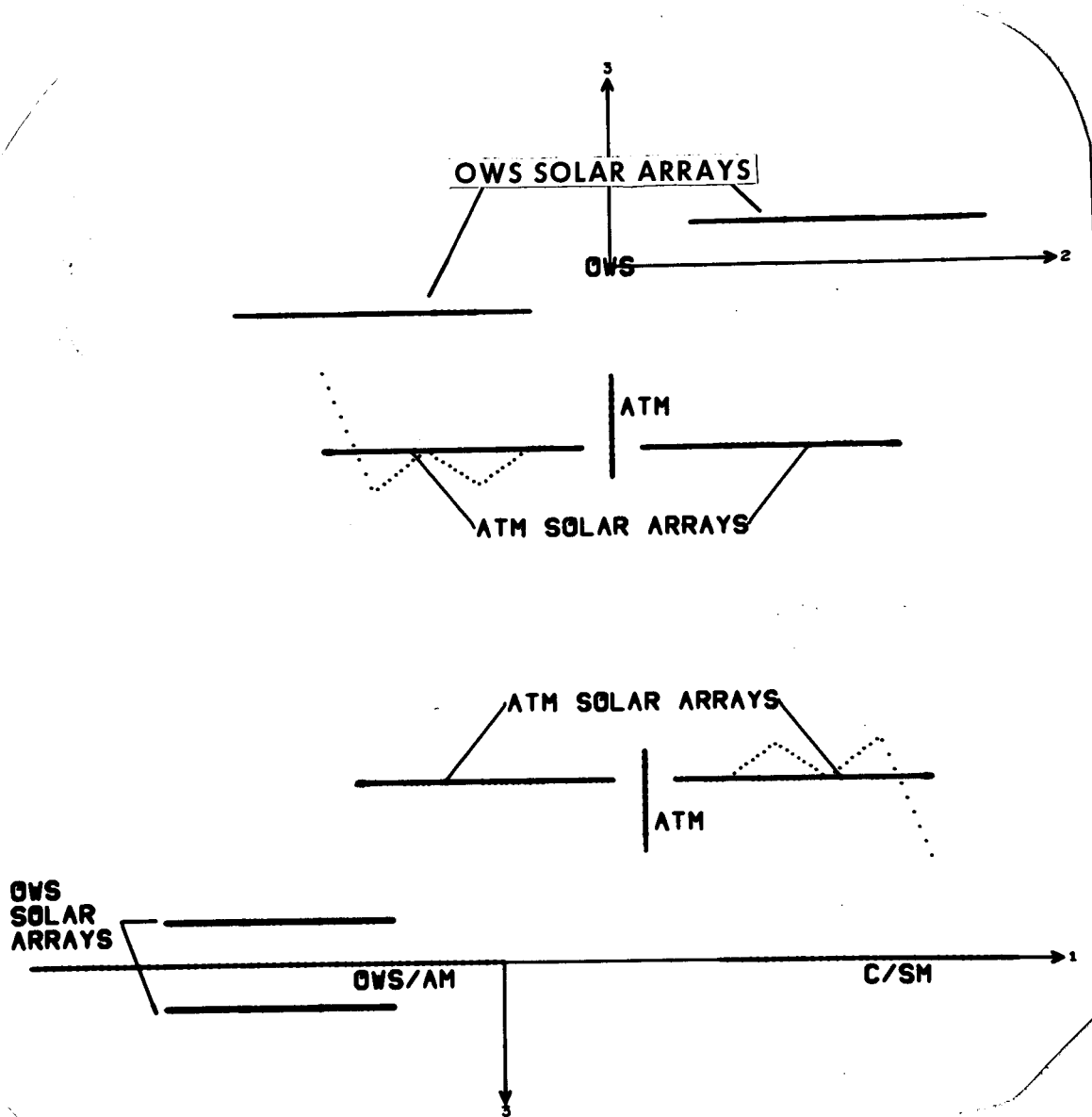
T. L. Bernstein  
 E. L. Bernstein  
 Fig. 6  
 1/10.7





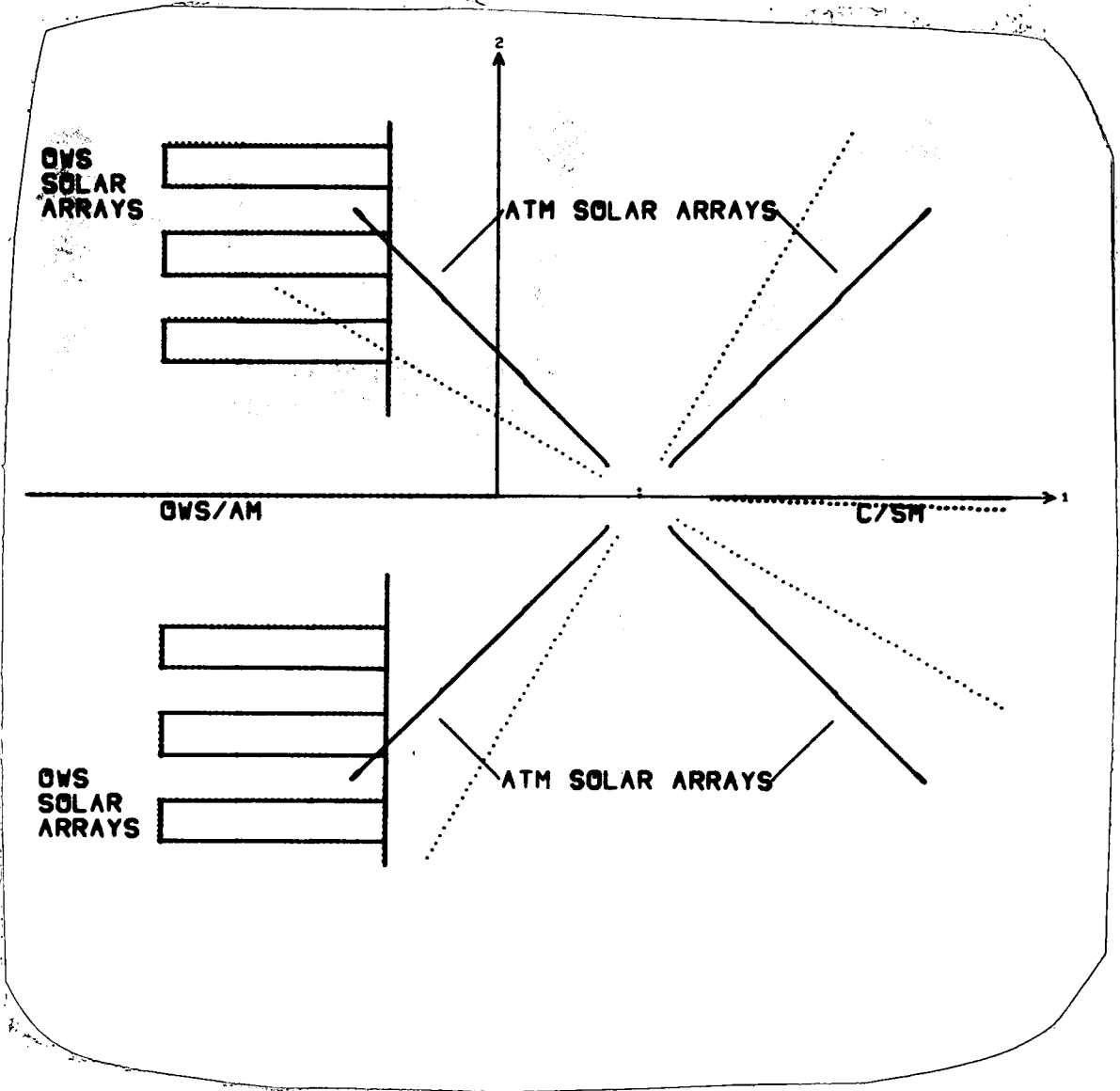
E. L. Bernstein

E. L. Bernstein  
Fig. 7



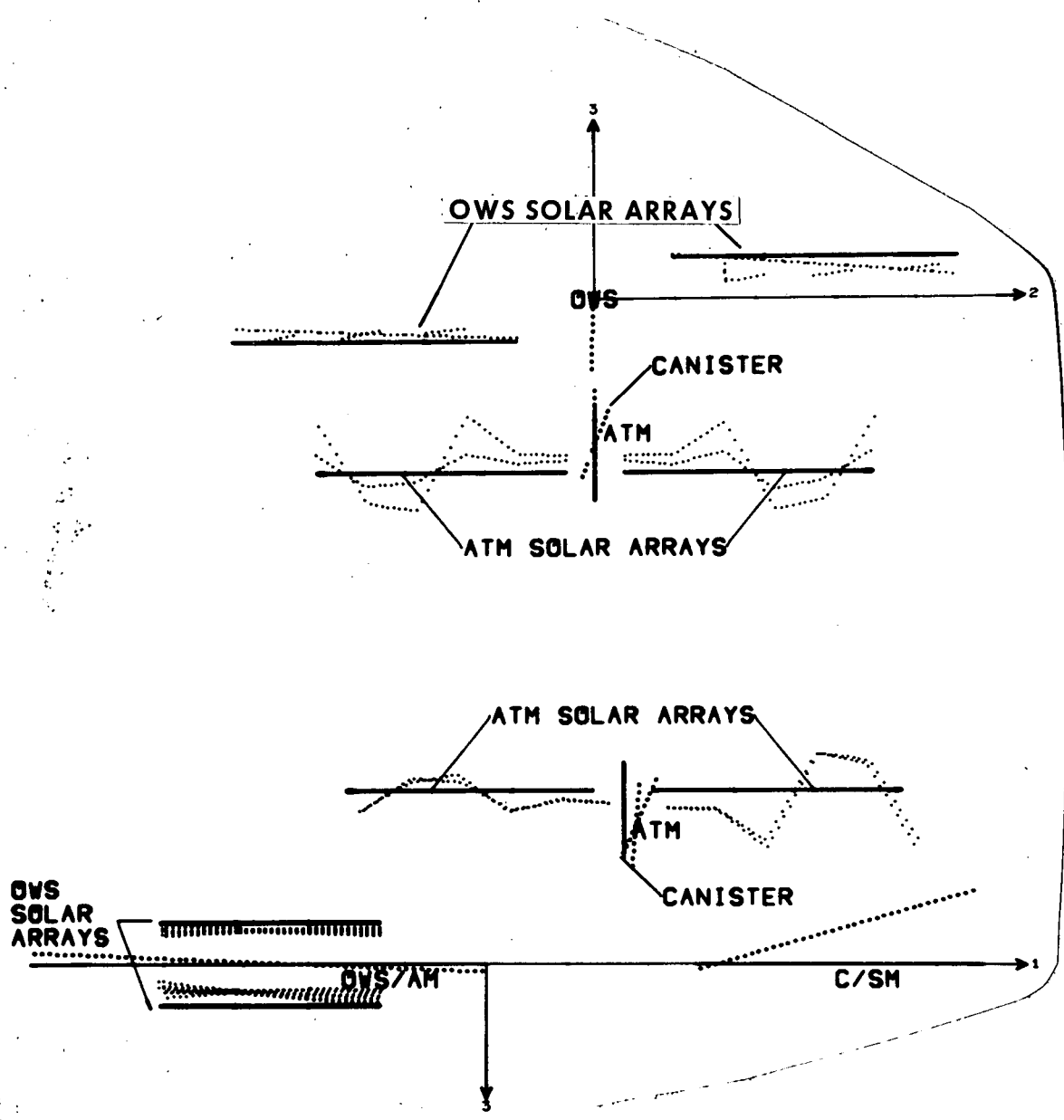
*E. L. Bernstein*

E. L. Bernstein  
Fig. 8/6 9



E.L. Bernstein

Fig. 9  
E. L. Bernstein  
Fig. 9



E. L. Bernstein  
 Fig. 10  
 176 11